REPORT DOCUMENTATION PAGE

Form Approved
OMB No. 0704-0188

1. REPORT DATE *(DD-MM-YYYY)*	2. REPORT TYPE	3. DATES COVERED *(From - To)*
1/1/0001	Journal Article - Journal Article	1/1/0001 - 1/1/0001

4. TITLE AND SUBTITLE
Molecular- and Domain-level Microstructure-dependent Material Model for Nano-segregated Polyurea

5a. CONTRACT NUMBER

5b. GRANT NUMBER

5c. PROGRAM ELEMENT NUMBER

6. AUTHOR(S)

5d. PROJECT NUMBER

5e. TASK NUMBER

5f. WORK UNIT NUMBER

7. PERFORMING ORGANIZATION NAME(S) AND ADDRESS(ES)
Clemson University Clemson SC 242

8. PERFORMING ORGANIZATION REPORT NUMBER

9. SPONSORING/MONITORING AGENCY NAME(S) AND ADDRESS(ES)
Office of Naval Research Arlington 46 242

10. SPONSOR/MONITOR'S ACRONYM(S)

11. SPONSOR/MONITOR'S REPORT NUMBER(S)

12. DISTRIBUTION/AVAILABILITY STATEMENT
1 1/1/0001 12:00:00 AM

13. SUPPLEMENTARY NOTES

14. ABSTRACT
Purpose – Polyurea is an elastomeric two-phase co-polymer consisting of nanometer-sized discrete hard (i.e. high glass transition temperature) domains distributed randomly within a soft (i.e. low glass transition temperature) matrix. A number of experimental investigations reported in the open literature clearly demonstrated that the use of polyurea external coatings and/or internal linings can significantly increase blast survivability and ballistic penetration resistance of target structures, such as vehicles, buildings and field/laboratory test-plates. When designing blast/ballistic-threat survivable

15. SUBJECT TERMS

16. SECURITY CLASSIFICATION OF:			17. LIMITATION OF ABSTRACT	18. NUMBER OF PAGES	19a. NAME OF RESPONSIBLE PERSON
a. REPORT	b. ABSTRACT	c. THIS PAGE			19b. TELEPHONE NUMBER *(Include area code)*
U	U				

The current issue and full text archive of this journal is available at
www.emeraldinsight.com/1573-6105.htm

Received 12 October 2012
Revised 5 February 2013
Accepted 15 April 2013

Molecular- and domain-level microstructure-dependent material model for nano-segregated polyurea

Mica Grujicic, Jennifer Snipes, Subrahmanian Ramaswami, Rohan Galgalikar, James Runt and James Tarter
Department of Mechanical Engineering, Clemson University, Clemson, South Carolina, USA

Abstract

Purpose – Polyurea is an elastomeric two-phase co-polymer consisting of nanometer-sized discrete hard (i.e. high glass transition temperature) domains distributed randomly within a soft (i.e. low glass transition temperature) matrix. A number of experimental investigations reported in the open literature clearly demonstrated that the use of polyurea external coatings and/or internal linings can significantly increase blast survivability and ballistic penetration resistance of target structures, such as vehicles, buildings and field/laboratory test-plates. When designing blast/ballistic-threat survivable polyurea-coated structures, advanced computational methods and tools are being increasingly utilized. A critical aspect of this computational approach is the availability of physically based, high-fidelity polyurea material models. The paper aims to discuss these issues.

Design/methodology/approach – In the present work, an attempt is made to develop a material model for polyurea which will include the effects of soft-matrix chain-segment molecular weight and the extent and morphology of hard-domain nano-segregation. Since these aspects of polyurea microstructure can be controlled through the selection of polyurea chemistry and synthesis conditions, and the present material model enables the prediction of polyurea blast-mitigation capacity and ballistic resistance, the model offers the potential for the "material-by-design" approach.

Findings – The model is validated by comparing its predictions with the corresponding experimental data.

Originality/value – The work clearly demonstrated that, in order to maximize shock-mitigation effects offered by polyurea, chemistry and processing/synthesis route of this material should be optimized.

Keywords Material model, Polyurea, Shock-mitigation

Paper type Research paper

1. Introduction

In the present work, an attempt is made to develop a chemical composition- and microstructure-dependent material model for polyurea in order to identify polyurea formulation and morphology which provide maximum shock-mitigation capability. Hence, the key aspects of the present work are:

The material presented in this paper is based on work supported by the Office of Naval Research (ONR) research contract entitled "Elastomeric Polymer-By-Design to Protect the Warfighter Against Traumatic Brain Injury by Diverting the Blast Induced Shock Waves from the Head", Contract Number 4036-CU-ONR-1125 as funded through the Pennsylvania State University. The authors are indebted to Dr Roshdy Barsoum of ONR for his continuing support and interest in the present work, and also to Professor G. Settles for stimulating discussions and friendship.

Multidiscipline Modeling in Materials and Structures
Vol. 9 No. 4, 2013
pp. 548-578

1573-6105
DOI 10.1108/MMMS-10-2012-0014

- polyurea;
- functional requirements for polyurea when used in blast-mitigation applications; and
- modeling of the mechanical response of polyurea under dynamic/blast-loading conditions.

These aspects will be briefly overviewed in the remainder of this section.

Polyurea

Polyurea is an elastomeric co-polymer that is formed by a rapid co-polymerization reaction between two groups:

(1) an isocyanate (an organic compound containing isocyanate —N═C═O group); and

(2) an amine (organic compound containing amine —NH2 group).

A schematic of this reaction is shown in Figure 1(a), where R is used to represent an aromatic functional group (e.g. di-phenyl methane), R' is used to denote an aromatic/aliphatic long chain functional group (e.g. poly-tetramethyleneoxide-di-phenyl) and U is used to indicate a urea linkage. The short co-polymerization/gel reaction time (typically less than a minute) enables polyurea synthesis to be achieved over a wide range of temperatures and humidity levels without significantly affecting material microstructure and properties, while additionally allowing conventional spraying processes to be used in the application of polyurea as a protective coating on target structures.

As shown schematically in Figure 1(b), polyurea chains contain two distinct types of segments:

(1) hard segments (HS), which are formed by highly polar (i.e. containing centers/poles of negative and positive charge) urea linkages (—NH—CO—NH—) and adjoining di-phenyl methane (C_6H_5—CH_2—C_6H_5) functional groups; and

(2) soft segments (SS), which consist of a series of aliphatic functional groups.

In bulk polyurea, strong hydrogen bonding between urea linkages of the adjacent chains (or between neighboring portions of the same chain) promotes microphase-segregation (self-assembly) of HS into the so-called nanometer-sized "hard (i.e. high glass-transition temperature, often crystallized) domains". A schematic of this process is shown in Figure 2 in which, to help identify hard domains, (blue) nitrogen atoms are shown as enlarged spheres. The remaining hard and the SS of the polyurea chains are fairly well-mixed and form the so-called "soft (i.e. low glass-transition temperature, amorphous) matrix". It should be noted that strong hydrogen bonding between HS, within the hard-domains, provides non-covalent inter-chain cross-linking. This is the reason that polyurea is often referred to as a thermo-plastically cross-linked elastomer. In addition, depending on the amount of higher functionality isocyanate present in the precursor, polyurea may contain different extents of covalent inter-chain cross-linking.

As far as the morphology of the hard domains is concerned, they are generally found to be of a ribbon shape with a characteristic diameter of ca. 10 nm and an aspect ratio of 20:1 or greater. An example of the domain-level polyurea microstructure is revealed using tapping-mode atomic force microscopy (AFM) as shown in Figure 3.

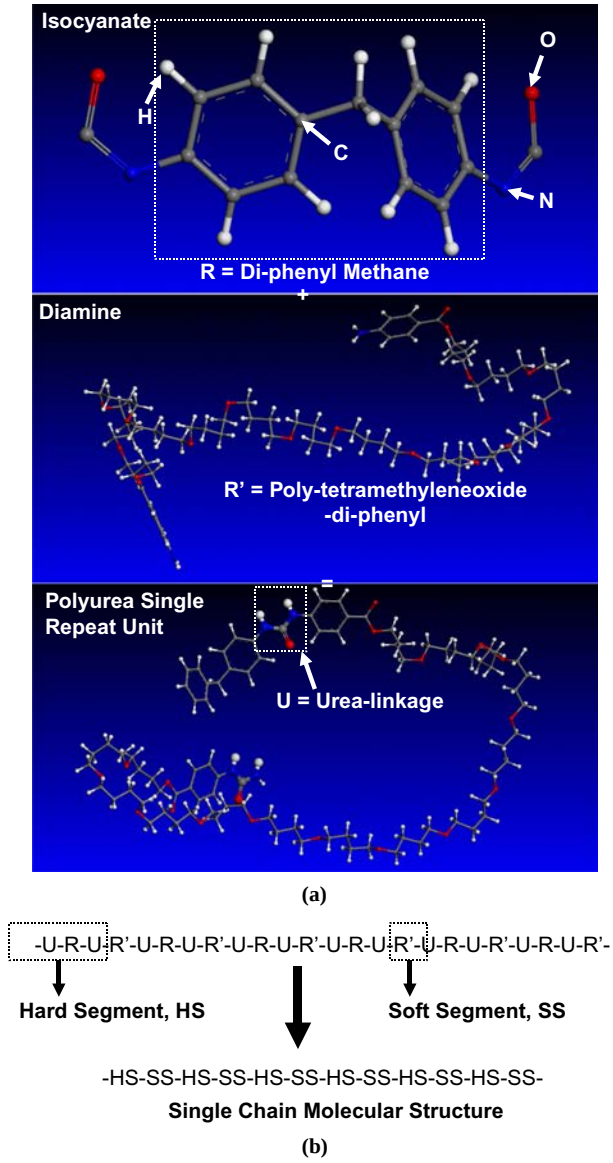

Figure 1.
(a) Co-polymerization reaction resulting in the formation of segmented polyurea and (b) simplified notation for polyurea structure using functional groups U (urea linkage), R (di-phenyl methane) and R′ (poly-tetramethy leneoxide-di-phenyl) and the corresponding definitions of HS and SS

While, typically, hard domains are present as discrete ribbon-shaped particulates, in some cases, they appear to be interconnected forming a contiguous network.

Based on the preceding descriptions of the polyurea molecular- and domain-level microstructures, this elastomeric material is usually referred to as being microphase-segregated and thermo-plastically cross-linked. Also, due to its two-phase microstructure, polyurea is often considered as an elastomeric-matrix based

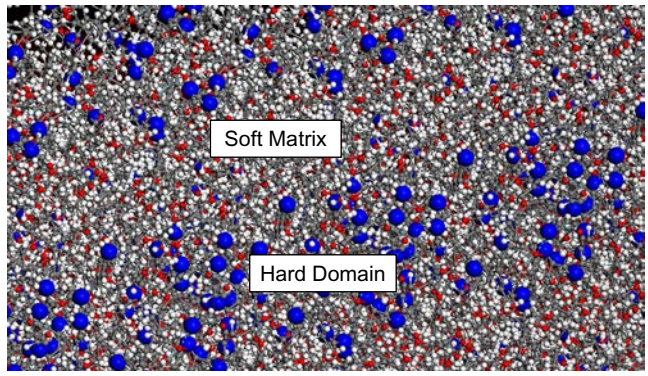

Note: To help identify hard domains, (blue) nitrogen atoms are shown as enlarged spheres

Figure 2.
Formation of hard domains and the soft matrix within nano-segregated bulk polyurea

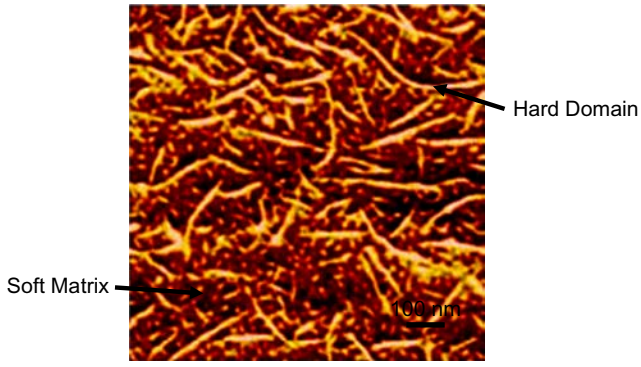

Figure 3.
A typical tapping-mode atomic force micrograph of polyurea showing its nano-segregated two-phase structure consisting of ribbon-like hard domains and a soft matrix

nanocomposite, in which nanometer-sized hard domains act both as stiff/strong reinforcements and as inter-chain linkages.

Various experimental investigations (Choi *et al.*, 2012) have established that microstructure and properties of polyurea are highly sensitive to the chemical composition and functionality of the precursors, synthesis route (e.g. solution-synthesis vs bulk synthesis) and synthesis conditions (e.g. temperature, humidity, etc.). However, while comprehensive investigations of these effects have been reported quite widely for polyurethanes and urethane-ureas (Garrett *et al.*, 2000, 2001, 2002, 2003; Bonart and Müller, 1974; Choi *et al.*, 2009; Hernandez *et al.*, 2007, 2008; Leung and Koberstein, 1985) similar reports related to polyurea are relatively scarce (Das *et al.*, 2007a, b, 2008). This state of affairs has been changed recently with the publication of the work conducted by Runt and co-workers (Castagna *et al.*, 2012).

In their work, Runt and co-workers (Castagna *et al.*, 2012) carried out a detailed experimental investigation of the effect of the soft-segment molecular weight (as governed by poly-tetra-methylene-oxide, PTMO segment length) on nanometer-scale microstructure of phase-separated, bulk-synthesized polyurea (containing a modified methylene diphenyl diisocyanate, mMDI, HS), as well as on

the state of hydrogen bonded associations, and soft-segment-chain dynamics. Application of tapping mode AFM clearly revealed that HS self-assemble into ribbon-like hard domains in the two high-soft-matrix-molecular-weight renditions of polyurea (P1000 and P650). On the other hand, the extent of hard-segment self-assembly was very low in the case of the third low-soft-matrix-molecular-weight rendition of polyurea (P250), suggesting that this material is effectively single-phase.

Through the use of small-angle X-ray scattering (SAXS), Runt and co-workers (Castagna *et al.*, 2012) showed that even in the case of P1000 and P650, phase segregation (i.e. formation of hard domains and soft matrix) was incomplete. In addition, it was found that as the molecular weight is lowered from 1000 g/mol in P1000 to 650 g/mol in P650, the extent of phase demixing was reduced. In addition, SAXS established an average interdomain spacing in P1000 and P650 to be around 7 nm.

Application of wide-angle X-ray diffraction (WAXD) suggested that within hard domains, ordering of urea linkages may take place, leading to the formation of crystalline-like structures.

The state of hydrogen bonding was probed using attenuated total reflectance-Fourier transform infra-red spectroscopy (ATR-FTIR). The results obtained revealed the presence of ordered, disordered, free and mixed hydrogen bonds associated with the carbonyl and N—H groups, which is fully consistent with the SAXS results for phase-segregated P1000 and P650.

Combined application of dynamic mechanical analysis (DMA) and dielectric relaxation spectroscopy (DRS) revealed the presence of two main soft-matrix-segment relaxation processes:

(1) the so-called "α relaxation process" which is associated with soft-matrix segments located farther away from the soft-matrix hard-domain interfaces; and

(2) the so-called "α_2 relaxation process" which is associated with the soft-matrix segments adjacent to the soft-matrix/hard-domain interfaces.

In addition to these more global types of relaxation processes, local relaxation processes are also observed, e.g. the so-called "γ relaxation process", which is associated with local motion of the ether-oxygen-containing functional groups in PTMO SS. A reduction in the soft-segment molecular weight from P1000 to P650 is found to slow down considerably the dynamics of these relaxation processes.

Polyurea has been found to display quite complex mechanical response under static and dynamic large-strain loading conditions, and this behavior is attributed to its complex hierarchical microstructure. The mechanical response is chiefly characterized by Ryan (1989) and Grujicic *et al.* (2010c):

- a high degree of material constitutive non-linearity;
- nearly perfect hyper-elastic response (i.e. only minor levels of the residual strains are observed upon unloading) under relatively low strain rates;
- highly pronounced temperature (and strain-rate) sensitivity; and
- strong pressure dependence arising from the nearly incompressible character of polyurea.

Use of polyurea in blast-mitigation applications

In recent years, polyurea external coatings and/or internal linings have been applied to structures to protect them against blasts produced by detonation of bombs, ordnance and improvised explosive devices (IEDs). This concept was first validated when the US Air Force demonstrated improved blast survivability of masonry buildings that were externally and internally sprayed with polyurea (Porter *et al.*, 2002). In addition to enhancing blast survivability of the masonry structures by delaying/preventing their structural collapse, polyurea coatings/linings were found to act as a "spall catcher" and prevent wall fragments/debris from entering the building interior. These fragments may often acquire quite high velocities and, hence, are often found to be the main cause of occupant injury or death. Further demonstration of the ability of polyurea coatings to improve blast survivability of target structures was provided by the US Navy's implementation of these coatings in the protection of its light tactical vehicles (e.g. US Marine Corp's High Mobility Multipurpose Wheeled Vehicle, HMMWV) and infrastructure (Matthews, 2004).

Recently, Roland and co-workers (Bogoslovov *et al.*, 2007) demonstrated that the application of polyurea front-face and back-face coatings can significantly enhance the ballistic-penetration resistance of steel test plates. By analyzing a comprehensive set of experimental results pertaining to the temporal and spatial evolution of the materials present in coated test structures during ballistic impact event and the polyurea time-dependent mechanical response as determined using the dielectric spectroscopy, Roland and co-workers (Bogoslovov *et al.*, 2007) concluded that phase transition of the polyurea from the rubbery to the glassy state is the most likely mechanism responsible for the observed beneficial effect of polyurea coatings on enhancing target-structure ballistic resistance. In addition, Roland and co-workers (Bogoslovov *et al.*, 2007) showed that in order to maximize the contribution of the rubbery-to-glassy state transition, chain segmental dynamics should be adjusted by placing (through chemical composition modifications) the polyurea glass transition temperature near but slightly below the test temperature. These findings were subsequently confirmed in a comprehensive computational investigation carried out by Grujicic *et al.* (2010c).

Based on the literature overview presented above, it appears that while the mechanism responsible for the increase in the ballistic penetration resistance of polyurea-coated test structure has been identified, the same could not be said for the mechanism(s) responsible for the superior shock-mitigation potential of polyurea. This point was clearly demonstrated in a series of publications reported by Grujicic *et al.* (2010a, b, 2011a, c, d, e, f, g, 2012a, b, d) and Grujicic and Pandurangan (2012), in which the blast-mitigation potential of polyurea was investigated in order to minimize the danger of traumatic brain injury of military personnel exposed to blast loading. The work of Grujicic *et al.* (2010a, b, 2011a, c, d, e, f, g, 2012a, b, d) and Grujicic and Pandurangan (2012) further demonstrated that one of the main reasons for the lack of understanding of the origin of superior blast-mitigation potential of polyurea is the incomplete understanding of microstructure-property relations in this class of materials. As will be discussed below, this incomplete understanding is reflected in the nature of the polyurea material models used in computer-aided engineering analyses of the interaction of blast waves with the target structure.

Polyurea material models available in the literature

A review of the literature carried out as part of the present work revealed the existence of six material models specifically developed for polyurea. These models will now be briefly reviewed and critically evaluated.

In the model proposed by Qi and Boyce (2005), the following physical aspects of polyurea microstructure and behavior are accounted for:

- the co-existence of soft-matrix and hard domains;
- the ability of the soft-matrix to undergo large reversible strains;
- the ability of hard-domains and hard-domain and soft-matrix interfaces to dissipate energy via rate-dependent inelastic-deformation processes; and
- a deformation-induced increase in the amount of soft-matrix (and the associated loss of material stiffness), due to disintegration of the hard-domains.

The model assumes that the material mechanical response can be represented by a structural element consisting of two parallel branches. The first branch represents the soft-matrix contribution and is represented using the Arruda-Boyce hyperelastic material model (Arruda and Boyce, 1993) while the second branch accounts for the contribution of the hard-domains and hard-domain/soft-matrix interfaces and is represented using an elastic/viscoplastic material formulation. A critical evaluation of this model carried out in the present work revealed two potential deficiencies:

(1) all the rate dependence has been attached to the hard domains (and the hard-domain/soft-matrix interfaces), i.e. the viscoelasticity in the soft matrix is not considered; and

(2) the relations pertaining to the evolution of volume fraction of the soft matrix and of the athermal shear strength of the hard domains are defined using phenomenological approaches which do not account for the underlying microstructural processes in polyurea and the relations used are essentially borrowed from the related filled-rubber-based materials.

Within the polyurea material model proposed by Amirkhizi *et al.* (2006), the hydrostatic response of the material is considered to be isotropic temperature-dependent geometrically non-linear/materially-linear elastic while the deviatoric response of the material is assumed to be time-dependent and treated using a geometrically-nonlinear/materially-linear isotropic viscoelastic formulation. To account for the aforementioned time-dependent character of the deviatoric material response, the deviatoric Cauchy stress, σ', is evaluated within the model by taking into consideration the entire deformation history of a given material point from the onset of loading. To account for the effect of temperature and pressure on the kinetics of relaxation processes responsible for the observed viscoelastic behavior, the concept of reduced time is utilized. Through the use of the reduced time concept, the effect of temperature is modeled by changing the time scale while leaving the material relaxation parameters constant and equal to their values at the reference temperature. To determine temporal evolution of the temperature, an adiabatic assumption is invoked, i.e. it is assumed that there is no heat transfer and that the rate of change of the local internal thermal energy is equal to the corresponding rate of dissipative work. Critical assessment of this model identified three points of concern:

(1) no consideration is given to the fact that polyurea is a two-phase material with distinct constitutive behavior of the two phases as well as of the interphase boundaries;

(2) the lack of objectivity under large rotations; and

(3) lack of inclusion of the so-called "stretch-induced" softening (i.e. a loss of material stiffness due to prior loading).

In the model proposed by Li and Lua (2009), polyurea is treated as an incompressible material. Hence, the model can only be used in deformation analyses in which the hydrostatic stress can be assessed through alternative means. For example, in the case of uniaxial-stress loading, the zero stress condition in the lateral directions enables the determination of the hydrostatic stress. As far as the material deviatoric response is concerned, it is modeled using a single structural element consisting of two parallel branches, one hyperelastic (based on the Ogden (1972)-type model and controlling material response under low deformation rates) and the other viscoelastic (modeled using a formulation similar to that used by Amirkhizi *et al.* (2006)). Critical assessment of this model identified that, with the exception of the problem related to the lack of objectivity, this model suffers from similar deficiencies as the one of Amirkhizi *et al.* (2006). In addition, as pointed out, the model entails the use of additional methods in order to assess the hydrostatic stress.

While the model proposed by Jiao *et al.* (2009) is quite similar to the Qi and Boyce (2005) model, and considers the presence of two branches, one hyperelastic and the other elastic/viscoplastic, the following main differences have been identified:

(1) the first branch is represented using the Neo-Hookean hyperelastic formulation;

(2) no account is given to the fact that this branch is associated with the soft matrix;

(3) neither soft-matrix strain amplification nor evolution of the soft-matrix volume fraction is considered; and

(4) the effect of hard-domain degradation and the associated loss of stiffness during deformation is also neglected.

Points (2) and (4) can also be identified as the main potential shortcomings of this model.

The model proposed by El-Sayed (2008) considers the presence of one hyperelastic-plastic and several viscohyperelastic branches, all connected in parallel. The hyperelastic response within each branch is modeled using an Ogden strain energy density function. The plastic (deviatoric + hydrostatic) response of the first branch is considered to be strain- and strain-rate hardenable while the viscoelastic response of the remaining branch(es) is treated using the Prony series formulism. The model also takes into account the plastic expansion or contraction of voids and therefore the stresses are appropriately modified to account for the effect of micro inertia (Ortiz and Molinari, 1992; Weinberg *et al.*, 2006). The following main concerns have been identified with regard to this model:

- a relatively large number of parameters and a need for extensive parameter identification efforts; and

- the model is of a generic type and does not include any unique microstructural or behavioral features of polyurea.

The last polyurea material model reported in the open literature is the one initially proposed by Grujicic *et al.* (2011b). Within this model, polyurea is treated as a (soft-matrix + hard-domains) two-phase, isotropic, hyper-elastic (with degradable elastic stiffness components) and rate-independent plastic material. Consequently, at small strains, the mechanical response of polyurea is completely reversible, i.e. no permanent changes in the material microstructure or residual strains are predicted. At larger strains, however, degradation/breakage of the hydrogen bonds within the HS of polyurea is assumed to give rise both to inelastic-deformation and stiffness-degradation effects. The model is mainly parameterized not by fitting a set of experimental data but rather using various material-property correlation analyses. The main concern regarding this model is that it is of a quasi-static nature and, hence, of limited utility with respect to its use in computer aided engineering analyses of various shock/ballistic-impact scenarios.

Main objective

While the polyurea material models overviewed above address a number of important microstructure/property relations in this material, two important aspects of this relationship are not accounted for:

(1) the effect of soft-segment molecular weight. As discussed earlier, the work of Runt and co-workers (Castagna *et al.*, 2012) clearly revealed that many aspects of material response are affected by the soft-segment molecular weight; and

(2) morphology, size, volume fraction and interconnectivity of hard domains within the soft matrix.

The effect of these microstructural parameters on the properties of polyurea has also been demonstrated in the work of Runt and co-workers (Castagna *et al.*, 2012). Consequently, the main objective of the present work is to develop a new polyurea material model (by extending one of the existing polyurea material models) which incorporates these two important effects.

Organization of the paper

Details regarding the development and parameterization of the new microstructure-sensitive polyurea material model are presented in Section 2. An analysis of planar longitudinal shock wave propagation within polyurea and of the role of different aspects of material microstructure in viscous dissipation of the strain and kinetic energy associated with the shock front (i.e. in the shock-mitigation performance) is presented in Section 3. The main conclusions resulting from the present work are summarized in Section 4.

2. Polyurea material model development

In this section, a detailed description is provided of the procedures used and of the governing equations developed during the construction of the new microstructure-dependent material model for polyurea. The starting point for the development of the new model is the polyurea material model originally developed by

Amirkhizi *et al.* (2006). This model was briefly overviewed in the previous section and some of its deficiencies were identified. Nevertheless, due to its mathematical simplicity and its ability to be relatively easily linked with the microstructure/property correlations established in the recent work of Runt *et al.* (Castagna *et al.*, 2012), this model was selected as the foundation for the newly developed model.

Within this model, deviatoric and hydrostatic components of the stress tensors are evaluated separately, and the total stress, at any point during the deformation history, is obtained by combining the two sets of stress components.

2.1 Deviatoric component of the stress

Linear hereditary integral formulation. Within the original model proposed by Amirkhizi *et al.* (2006), the deviatoric response of polyurea is assumed to be rate/time-dependent and is treated using a geometrically-nonlinear/materially-linear isotropic viscoelastic formulation. This formulation is retained in the present work, except that key parameters are converted into microstructure-dependent quantities. To account for the aforementioned time-dependent character of the deviatoric material response, the deviatoric Cauchy stress tensor, σ', is evaluated within the model by taking into consideration the entire deformation history of a given material point from the onset of loading at $t = 0$ to the current time, t, through the use of the following linear hereditary integral:

$$\sigma'(t) = 2\int_0^t G(t,\tau)D'(\tau)d\tau \tag{1}$$

where G is the time-dependent shear relaxation modulus, D' is the deviatoric part of the deformation-rate tensor and τ is a time variable ($0 \leq \tau \leq t$). The deviatoric part of the deformation-rate tensor is computed as $D' = D - 1/3*\mathrm{tr}(D)*I$, where tr denotes trace operator and I an identity tensor. The total deformation-rate tensor, D is in turn defined as $D = sym\,(\dot{F}F^{-1})$, where sym, the raised dot and superscript " -1", are used to denote, respectively, the symmetric part, the time derivative, and the inverse of a second order tensor and F denotes the deformation gradient.

The shear relaxation modulus is next expressed, at the reference temperature T_{ref}, using a Prony series expansion to get:

$$\sigma'(t) = 2G_\infty(T_{ref})\int_0^t \left(1 + \sum_{i=1}^{n} p_i \exp\left(\frac{-(t-\tau)}{q_i}\right)\right) D'(\tau)d\tau \tag{2}$$

where G_∞ is the "long-term" shear modulus (i.e. the value of the shear modulus after infinitely long relaxation time), n is the number of terms in the Prony series exponential-type relaxation function and p_i and q_i are, respectively, the strength and the relaxation time of each Prony series term.

The effect of temperature is included in two ways (Pipkin, 1972):

(1) it is first recognized that the long-term shear modulus scales nearly linearly with a T/T_{ref} ratio, where T is the instantaneous temperature; and

(2) it is also acknowledged that due to the higher level of vibrational/thermal energy present at higher temperatures, the rates of molecular relaxation processes are increased.

To account for the increased rate of relaxation processes at high temperatures, the so-called "time-temperature superposition" concept is utilized (Williams *et al.*, 1955). Within this concept, it is assumed that the same effect of molecular relaxation attained at higher temperatures can be achieved by extending the relaxation time at the reference temperature. As a result, a new time scale (generally referred to as the reduced time scale) is introduced as:

$$\xi(t) = \int_0^t \frac{d\tau}{a(T(\tau))} \tag{3}$$

where $a(T)$ is a time-temperature shift function that depends on the instantaneous temperature, reference temperature and the material-microstructure-dependent glass transition temperature T_g as:

$$a(T) = 10^{A(T_g)(T-T_{ref})/[B(T_g)+T-T_{ref}]} \tag{4}$$

where $A(T_g)$ and $B(T_g)$ (normally treated as material constants) are considered, in the present work, as material-microstructure-dependent functions.

In addition to temperature, pressure also has a pronounced effect on the kinetics of relaxation of molecular level processes. This effect is generally related to the presence of free-volumes within polymeric materials. Free-volumes facilitate relaxation processes and increase their rate. Under pressure, the free-volume content is reduced which leads to a reduction in the rates of stress relaxation processes. Since this effect is analogous to that associated with a reduction in temperature, the effect of pressure, P, is incorporated by utilizing a pressure-modified instantaneous temperature in the time-temperature shift function as:

$$a(T, P) = a(T - C_{tp}P) \tag{5}$$

where C_{tp} is an experimentally determinable pressure-based temperature correction coefficient.

By combining equations (1)-(5), the following expression is obtained for the time-dependent Cauchy stress tensor:

$$\sigma'(t) = \frac{2G_\infty(T_{ref})}{T_{ref}} \int_0^t T(\tau)\left(1 + \sum_{i=1}^{n} p_i \exp\left(\frac{-(\xi(t) - \xi(\tau))}{q_i}\right) D'(\tau)\right) d\tau \tag{6}$$

It should be noted that through the use of the reduced time concept, the effect of temperature and pressure is modeled by changing the time scale while leaving the material relaxation parameters p_i and q_i temperature-/pressure-invariant and equal to their values at the reference temperature and zero-pressure. This assumption is justified only under the conditions that the deviations in temperature and pressure from their reference values affect solely the rate, but not the mechanism, of molecular-level relaxation processes. It should be also recognized that, in the present work, relaxation parameters are not treated as constants but rather as material-microstructure-dependent quantities.

A careful examination of equation (6) reveals that the deviatoric stress tensor defined by this equation is not objective and hence its use is strictly valid only under conditions of small rotations. These conditions are generally met under weak blast-loading

conditions (as encountered in the problem of traumatic brain injury, of primary concern in the present work) but are often violated in the case of ballistic impact and penetration of polyurea-coated target structures. For equation (6) to become objective under large-rotation cases, it must be properly modified by replacing the deviatoric stress rate (in the integrand of equation (6)) by one of its objective counterparts. Since this modification is of a pure kinematic nature, it can be readily implemented but the resulting formulation is associated with a significantly higher computational cost. Due to the fact that the present work is primarily concerned with the mechanical response of polyurea under weak blast-loading conditions, the extension of the present material model into the large-rotation range is deemed unnecessary.

Energy dissipation and temporal evolution of temperature. Examination of equation (6) reveals that in order to determine temporal evolution of the deviatoric stress tensor, one must also determine temporal evolution of the temperature. In the course of loading (and unloading), temperature is changing due to viscous dissipation of the material strain energy. To determine temporal evolution of the temperature within the model, an adiabatic assumption is invoked, i.e. it is assumed that the heat transfer is absent and that the rate of change of the local internal thermal energy is equal to the corresponding rate of dissipative work, W_d, as:

$$C_v \frac{\partial T}{\partial t} = \frac{\partial W_d}{\partial t} \tag{7}$$

where C_v is the (volumetric) constant volume specific heat.

The dissipative work can be defined by integrating, over the deformation history, the double-dot product of the stress tensor and the dissipative/relaxation portion of the deformation-rate tensor. Differentiation of the resulting relation with respect to time yields:

$$\frac{\partial W_d}{\partial t} = 2G_{\infty} \frac{T(t)}{T_{ref}} \sum_{i=1}^{n} \frac{p_i}{q_i} \boldsymbol{\varepsilon}_d^i(t) : \boldsymbol{\varepsilon}_d^i(t) \tag{8}$$

where $\boldsymbol{\varepsilon}_d^i$ is the component of the dissipative strain tensor associated with the relaxation branch i defined as:

$$\boldsymbol{\varepsilon}_d^i(t) = \int_0^t \exp\left(\frac{-(\xi(t) - \xi(\tau))}{q_i}\right) \mathbf{D}'(\tau) d\tau \tag{9}$$

The rate of change of temperature, $\partial T/\partial t$, can be computed by combining equations (7)-(9) and the temperature updated using a simple forward differencing scheme $T(t + \Delta t) = T(t) + (\partial T/\partial t)\, \Delta t$.

Numerical integration. At the first glance, evaluation of the deviatoric stress tensor via equation (6) appears straightforward. However, this would require that equation (6) be re-integrated from the onset of loading at $t = 0$, at each time step. This would cause an extremely high computational cost and demand prohibitively large data storage resources. Fortunately, as will be shown below, the specific form (i.e. the Prony series type) of the shear relaxation modulus function enables the integration to be carried out in a computationally less demanding manner. Using the notion of the dissipative strain tensor components, equation (9), the hereditary integral at time t given by equation (6) can be rewritten as:

$$\boldsymbol{\sigma}'(t)=\frac{2G_{\infty}(T_{ref})}{T_{ref}}\times\left[\int_0^t T(\tau)\mathbf{D}'(\tau)d\tau+\sum_{i=1}^{n}p_i\int_0^t T(\tau)\exp\left(\frac{-(\xi(t)-\xi(\tau))}{q_i}\right)\mathbf{D}'(\tau)d\tau\right] \tag{10}$$

while the same integral at time $t + \Delta t$ can be written as:

$$\boldsymbol{\sigma}'(t+\Delta t)=\frac{2G_{\infty}(T_{ref})}{T_{ref}}\times\left[\int_0^{t+\Delta t} T(\tau)\mathbf{D}'(\tau)d\tau+\sum_{i=1}^{n}p_i\int_0^{t+\Delta t} T(\tau)\exp\left(\frac{-(\xi(t+\Delta t)-\xi(\tau))}{q_i}\right)\mathbf{D}'(\tau)d\tau\right] \tag{11}$$

Through simple mathematical manipulations of equations (10) and (11), one can show that:

$$\boldsymbol{\sigma}'(t+\Delta t)=\boldsymbol{\sigma}'(t)+\Delta\boldsymbol{\sigma}'(t,\Delta t) \tag{12}$$

where $\Delta\boldsymbol{\sigma}'(t, \Delta t)$ is the net correction to the deviatoric stress tensor in the $(t, t + \Delta t)$ time period, and is given by:

$$\Delta\boldsymbol{\sigma}'(t,\Delta t)=\frac{2G_{\infty}(T_{ref})}{T_{ref}}\times\left[\int_t^{t+\Delta t} T(\tau)\mathbf{D}'(\tau)d\tau+\sum_{i=1}^{n}p_i\int_t^{t+\Delta t} T(\tau)\exp\left(\frac{-(\xi(t)+\Delta\xi-\xi(\tau))}{q_i}\right)\mathbf{D}'(\tau)d\tau-\sum_{i=1}^{n}p_i\left(1-\exp\left(\frac{-\Delta\xi}{q_i}\right)\right)\int_0^t T(\tau)\exp\left(\frac{-(\xi(t)-\xi(\tau))}{q_i}\right)\mathbf{D}'(\tau)d\tau\right] \tag{13}$$

Examination of equation (13) reveals that in order to compute $\Delta\sigma'(t, \Delta t)$, one must determine and save as material state variables $6n$ integrals pertaining to the product of the instantaneous temperature and the relaxation-branch-specific dissipation function $\exp[-(\xi(t) - \xi(\tau))/q_i]$ (as contained in the last term on the right-hand side of equation (13)). As far as the other two terms on the right-hand side of equation (13) are concerned, they can be readily evaluated using numerical integration since the range of integration is small $(t, t + \Delta t)$. Thus, the deviatoric stress can be updated by simply adding the stress correction to the stress values evaluated at the end of the previous time increment.

2.2 Hydrostatic component of the stress

Within the original model of Amirkhizi *et al.* (2006), the hydrostatic response of polyurea is considered to be isotropic, temperature-dependent, geometrically non-linear/materially-linear elastic. This formulation was not adopted in the present work since our prior molecular-level simulation work (Grujicic *et al.*, 2012c) clearly revealed that hard domains can undergo irreversible volumetric changes when subjected to blast or ballistic high-rate loading. Consequently, the hydrostatic response

of polyurea is considered to be of an isotropic, temperature- and microstructure-dependent, geometrically non-linear/materially-linear elastic and linearly strain-hardening hydro-plastic character.

The elastic portion of the material volumetric response is modeled using the following pressure relation (Amirkhizi *et al.*, 2006):

$$P = -K_{el}(T)\frac{\ln(J)}{J}; \quad where \;\; K_{el}(T) = K_{el}(T_{ref}) + m_{el}(T - T_{ref}) \tag{14}$$

where K_{el} is the elastic bulk modulus and m_{el} a material parameter quantifying temperature sensitivity of the elastic bulk modulus.

As far as the plastic volumetric response of polyurea is concerned, it is defined by two temperature – material-microstructure- and curing-temperature-dependent quantities:

(1) a yield pressure, $p_y\,(T)$; and

(2) a plastic tangent-bulk modulus, $K_{pl}\,(T)$.

Temperature dependencies of these two parameters are assumed to be given by the same type of linear functional relationship as that one used for $K_{el}\,(T)$ in equation (14).

In accordance with standard practice (Grujicic *et al.*, 2006), 95 percent of the work of volumetric plastic deformation is assumed to be dissipated. The rate of this energy dissipation is next combined with the aforementioned visco-elastic dissipation rate and used to track temporal evolution of temperature.

2.3 Parameterization and implementation of the model

In this section, available molecular modeling and experimental data are used to parameterize the newly developed polyurea material model. Examination of the key equations defining the new model reveals the following material-model parameters: $G_\infty(T_{ref})$, $p_i\,(T_{ref})$, $q_i\,(T_{ref})$ $(i = 1, n)$, T_g, $K_{el}\,(T_{ref})$, $p_y\,(T_{ref})$, m_y, $K_{pl}\,(T_{ref})$, and m_{pl}. In accordance with the details of the newly developed material model, these parameters are treated not as constants but rather as polyurea microstructure- and synthesis-condition-dependent quantities.

Deviatoric viscoelastic spectrum. In the original polyurea material model of Amirkhizi *et al.* (2006), the time-dependent character of the material's purely deviatoric response is accounted for through four Prony-series terms. A functional relationship between the viscoelastic relaxation strength and the logarithm of the corresponding relaxation time at the reference temperature (298 K) for these four terms is shown in a bar-graph in Figure 4. Numeric labels are shown in this figure to indicate the order of the Prony-series terms used by Amirkhizi *et al.* (2006). As discussed in our previous work (Grujicic *et al.*, 2011d), the four relaxation terms can be associated with the following molecular-level relaxation processes:

(1) the fastest relaxation process, term 4, is associated with the chain side-group motions such as the motion of the ether-oxygen-containing functional groups in PTMO SS. Since the relaxation time is very short, this relaxation process can be considered as being fully completed at the characteristic time scales associated with either blast or ballistic impact events;

(2) term 3 is associated with the unconstrained-chain segmental dynamics in the portion of the soft-matrix which is further away from the

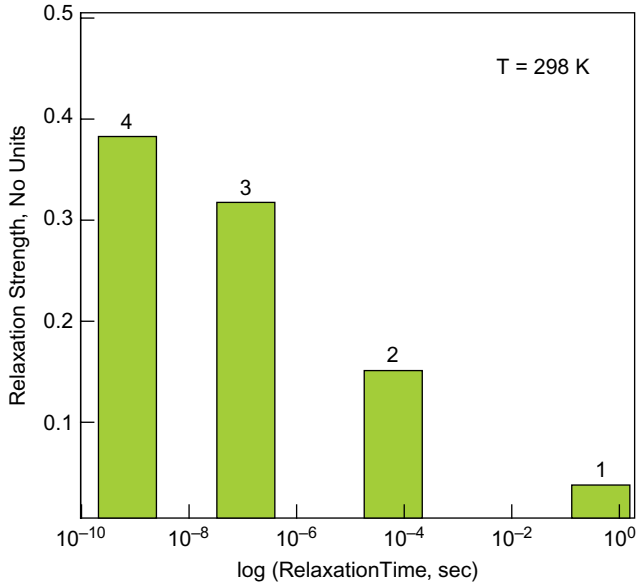

Note: Numerical labels are used to denote the order of four terms as initially specified by Amirkhizi *et al*. (2006)

Figure 4.
Polyurea viscoelastic spectrum consisting of four Prony-series terms as determined by Amirkhizi *et al.* (2006)

soft-matrix/hard-domain interfaces, and is commonly referred to as the α process. Immobilization of this viscoelastic relaxation branch is believed to be responsible for the rubbery-to-glassy transition in polyurea soft-matrix;

(3) term 2 is associated with the constrained-chain segmental dynamics in the portion of the soft-matrix which is adjacent to the soft-matrix/hard-domain interfaces, and is commonly referred to as the α_2 process; and

(4) the slowest relaxation process, term 1, is associated with a larger-scale molecular motion (e.g. translational and/or rotational motions of the hard-domains as a whole).

This relaxation mode may make a major contribution to the (lower-frequency) vibrational-damping capacity of polyurea but possesses quite small relaxation strength in the case of polyurea studied by Amirkhizi *et al.* (2006). In addition, due to its relatively long relaxation time (and small relaxation strength), this mode is not expected to play a significant role in the ability of this material to mitigate shock-loading or ballistic impact. Consequently, this term has been given relatively minor consideration in the present work.

The effect of soft-segment molecular weight on the viscoelastic spectrum. While the relaxation strength and relaxation time parameters associated with the four Prony-series viscoelastic terms were treated as constants in the original model of Amirkhizi *et al.* (2006), the work of Runt and co-workers (Castagna *et al.*, 2012) clearly revealed that these parameters are functions of the soft-segment molecular weight. By employing a post-processing data-reduction analysis to the DMA and DRS data reported

by Castagna *et al.* (2012), functional relationships are established between the relaxation strength and logarithm of the relaxation time on the one hand, and the soft-segment molecular weight on the other. These functional relationships are shown in Figure 5(a) and (b), respectively. Examination of the results depicted in these figures reveals that:

(1) the relaxation time for the γ process (process 4) is not significantly affected by the polyurea soft-segment molecular weight. However, the relaxation strength increases as soft segment molecular weight decreases. These findings are consistent with:
   - the local character of the associated relaxation process which is expected not to be significantly affected by the length of the polyurea SS; and
   - with the fact that as the soft segment molecular weight is reduced, the extent of nano-phase-segregation is also reduced, resulting in a larger volume fraction of the soft phase.

(2) the α relaxation process (process 3) is found to become more sluggish and more intense as the soft segment molecular weight is decreased. These findings are consistent with the fact that as the soft-segment molecular weight is reduced, the volume fraction of the soft-matrix containing unconstrained chain segments is increased while the segments themselves become more rigid and less compliant due to the configurational-entropy effects;

(3) the α_2 relaxation process (process 2) is observed to become more sluggish and less intense as the soft segment molecular weight is decreased. The observed reduction in the relaxation rate can again be attributed to the effect of increased rigidity and the contributions of the configurational-entropy effects. As far as the reduced relaxation strength is concerned, it is consistent with the fact that as the soft-segment molecular weight is reduced, the volume fraction of the soft-matrix containing constrained chain segments is also reduced due to the associated lower extent of nano-phase-segregation; and

(4) as far as relaxation branch 1 is concerned, Figure 5(b) shows that the associated relaxation process is essentially unaffected while Figure 5(a) shows that the relaxation strength decreases significantly with the decrease in the soft-segment molecular weight.

This finding is fully consistent with the fact that this relaxation process is related to the motion of the HS as a whole and to the fact that in the polyurea rendition with the lowest soft-segment molecular weight, extremely small fraction of hard-domains is generally observed.

The effect of curing temperature on the viscoelastic spectrum. To make the problem at hand more complicated, relaxation strengths of the viscoelastic branches 2 and 3 are not only affected by the soft segment molecular weight but also by polyurea synthesis conditions (primarily by the curing temperature, humidity and the solution/bulk synthesis route). In the present work, an attempt is made to only include the effect of polyurea curing temperature (by post-processing experimental data generated in the work of Runt and co-workers (Castagna *et al.*, 2012)). While the effects of other polyurea-synthesis conditions on the material microstructure can be significant, at present, experimental data available in the open literature is incomplete, rendering a quantitative treatment of these

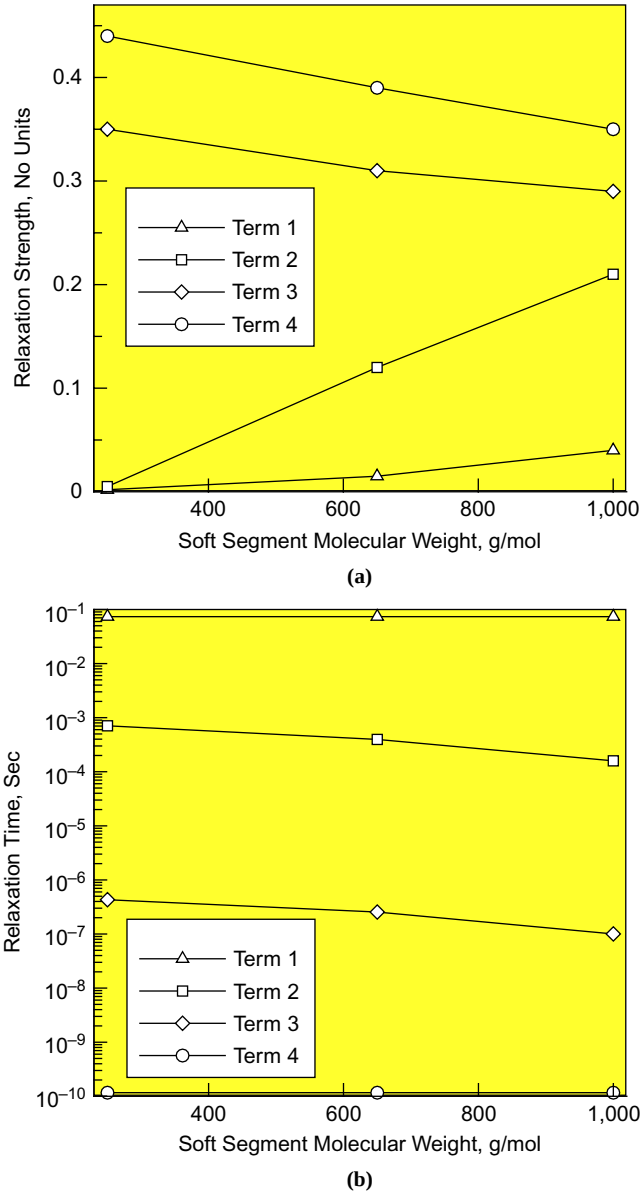

Figure 5.
The effect of the polyurea soft segment molecular weight, at 298 K, on (a) the relaxation strength and (b) the relaxation time associated with the four viscoelastic deviatoric relaxation processes

effects impractical. The combined effects of soft segment molecular weight and polyurea curing temperature on the strength of the α_2 (process 2) and α (process 3) relaxation processes are shown as contour plots in Figure 6(a) and (b), respectively. Examination of Figure 6(a) reveals that the α_2 relaxation strength increases with an increase in curing temperature, and that this increase is fairly insensitive to the magnitude of the soft-segment molecular weight. Furthermore, the effect of the curing temperature in

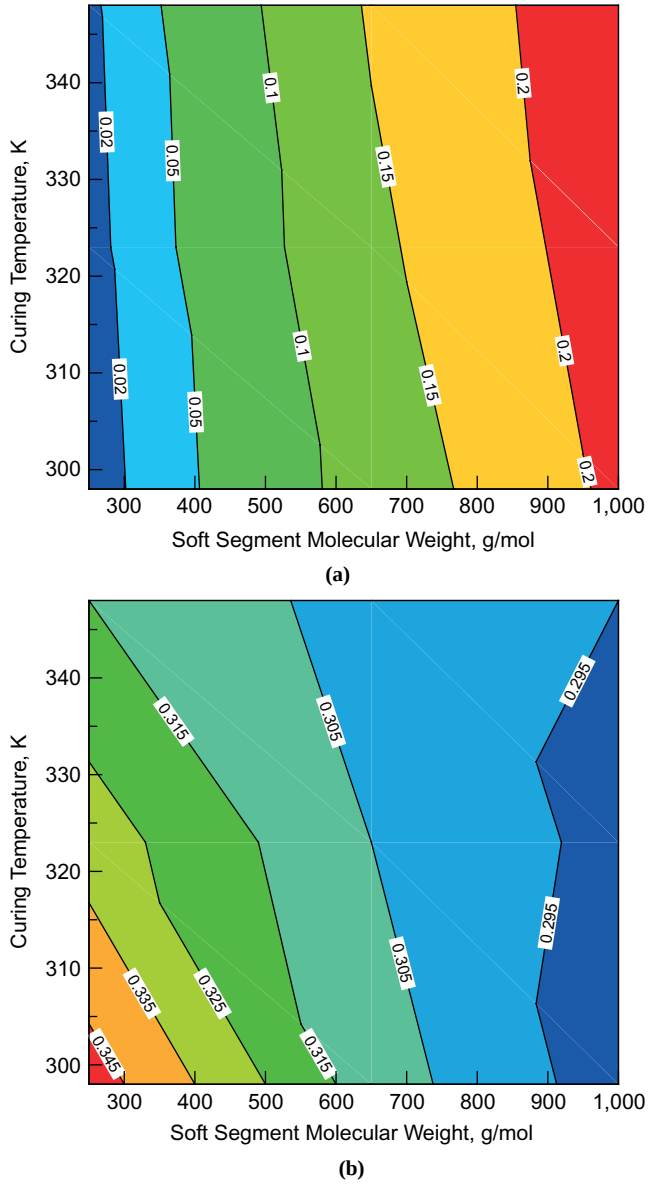

Figure 6.
The effect of the polyurea soft segment molecular weight and curing temperature on the strength of (a) the α_2 relaxation process and (b) the α relaxation process at 298 K

the range examined is substantially smaller than the corresponding effect associated with the investigated range of the soft-segment molecular weight. Examination of Figure 6(b) reveals that, as the curing temperature is increased, the α process relaxation strength decreases, remains fairly unaffected and slightly increases, at the lowest, intermediate and highest values of the soft-segment molecular weight, respectively. As far as the effect of curing temperature on the relaxation time of the α_2 and α relaxation processes

is concerned, it is found to be quite small (the results not shown for brevity). Also, the effect of curing temperature on the relaxation processes 1 and 4 was found to be inconclusive and, hence, it is assumed here that the p and q values related to these processes are insensitive to the polyurea curing temperature.

Temperature effect on the shear and bulk moduli. Temperature dependence of the bulk modulus has been previously defined by equation (14). Parameter m_{el} used in this equation was assigned a value of -0.015 GPa/K by Amirkhizi *et al.* (2006). Due to lack of relevant experimental and/or molecular-modeling data, this parameter was treated in the present work as being constant and equal to the foregoing value. As far as the temperature dependence of the long-term shear modulus is concerned, it was assumed, as stated earlier, to scale linearly with the T/T_{ref} ratio.

The values for G_∞ (T_{ref}) and K_{el} (T_{ref}) and the procedures used for their assessment can be found in our previous work (Grujicic *et al.*, 2011b).

Volumetric inelastic behavior. As mentioned earlier, one of the major deviations of the present polyurea material model from that presented by Amirkhizi *et al.* (2006) is the way the hydrostatic component of the stress is handled. In the present work, following our prior molecular-level computational analyses (Grujicic *et al.*, 2012c), it was assumed that, under blast and ballistic loading conditions, hard domains can undergo volumetric plastic/inelastic deformation (which may result in, at least partial, crystallization of the hard-domain material).

As explained earlier, hard-domains are formed during a micro-phase segregation process from fully mixed polyurea as a result of strong hydrogen bonding between urea linkages of the neighboring chains. Hard domains are characterized by a relatively high (ca. 250°C) glass-transition temperature and are often found to contain some fraction of the crystalline phase in the as-cast condition. Due to a large difference between T_g and the room temperature, one does not expect progressive thermally-activated crystallization of hard-domains at room-temperature to occur. However, strain-induced crystallization of hard-domains is still possible considering the fact that hard-domains are often found to re-orient themselves, under loading, in the principal direction of deformation (morphological texture). This re-orientation has been found, in our molecular-level simulation work (Grujicic *et al.*, 2012c), to be accompanied by additional internal reordering/crystallization of the hard-domains. Experimental evidence for this strain-induced hard-domain crystallization has been offered by Sheth *et al.* (2004). Furthermore, in the work of Runt and co-workers (Castagna *et al.*, 2012), it was observed that an increase in the soft-segment molecular weight and/or curing temperature leads to an initial degree of order (i.e. the initial extent of crystallization) within the hard-domains.

The hydrostatic stress model for polyurea presented in the previous section is characterized by three material-model parameters:

(1) the elastic bulk modulus, K_{el} (T_{ref});

(2) the hydrostatic yield pressure, p_y (T_{ref}); and

(3) the plastic tangent-bulk modulus, K_{pl} (T_{ref}).

By combining the computational results presented by Grujicic *et al.* (2012c) and the experimental findings reported by Runt and co-workers (Castagna *et al.*, 2012), functional relationships are established between the hydrostatic material-model parameters, on the one hand, and the soft-segment molecular weight and curing

temperatures on the other. These functional relations are shown using contour plots in Figure 7(a)-(c), respectively. Examination of Figure 7(a) and (b) reveals that both an increase in the soft-segment molecular weight and an increase in curing temperature give rise to an increase in polyurea hydrostatic elastic stiffness and strength. This finding is fully consistent with the fact that high molecular weight of SS and high curing temperature both increase the extent of nano-segregation (i.e. volume fraction of the hard phase) and the extent of initial-ordering/crystallization in the hard domains. As far as the plastic bulk modulus is concerned, Figure 7(c), it is found to decrease with an increase in either the soft-segment molecular weight or the curing temperature. This finding simply suggests that in hard domains with a lower degree of initial ordering/crystallization, the effects of "strain hardening" are more pronounced.

Glass transition temperature. The combined effects of the soft segment molecular weight and the curing temperature on the polyurea glass transition temperature is shown in Figure 8. Examination of this figure reveals that as the soft segment molecular weight is reduced the glass transition temperature increases and does so at a progressively higher rate. As far as the effect of curing temperature is concerned, the glass transition

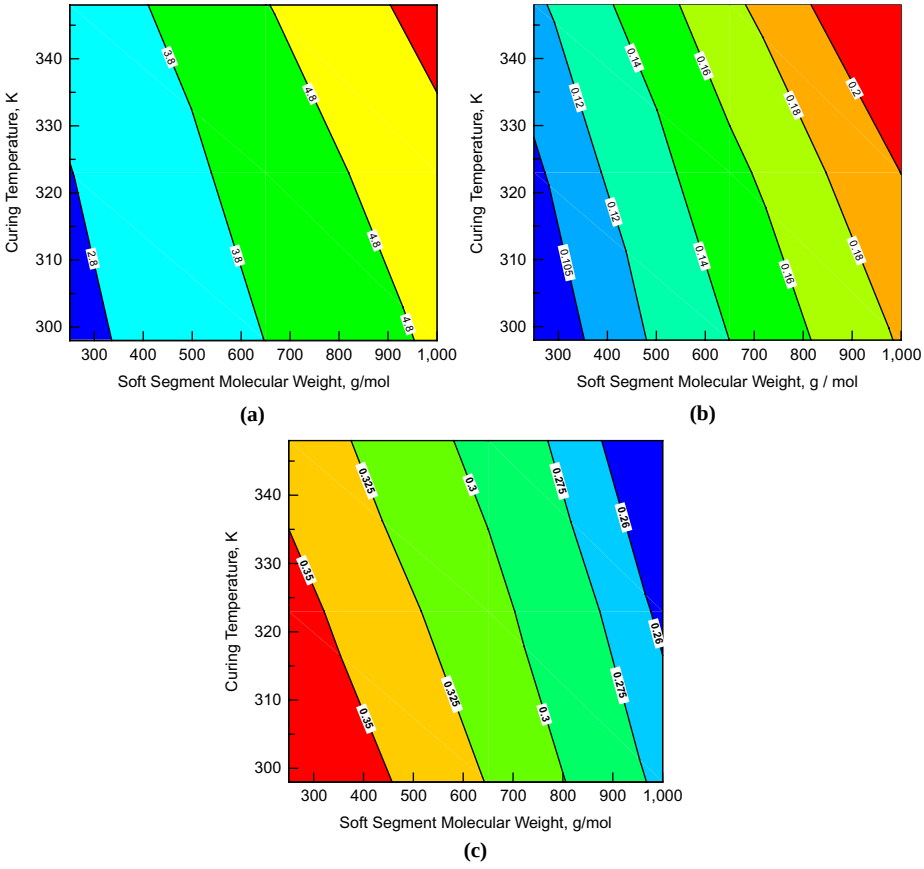

Figure 7.
The effect of the polyurea soft segment molecular weight and curing temperature on (a) the elastic bulk modulus K_{el} (GPa), (b) the yield pressure p_y (MPa) and (c) plastic tangent-bulk modulus, K_{pl} (GPa), at T = 298 K

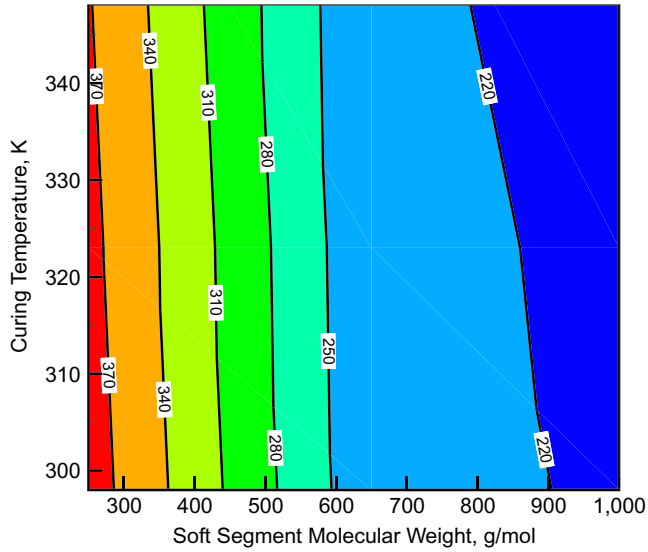

Figure 8.
The effect of the polyurea soft segment molecular weight and curing temperature on the glass transition temperature

temperature decreases with an increase in the curing temperature, and this effect is more pronounced in the case of low soft segment molecular weight polyurea.

Implementation of the model into a user material subroutine. The material model developed and parameterized above is implemented into the user material subroutine VUMAT of ABAQUS/Explicit (Dassault Systems, 2010), a commercial finite element code. This subroutine is called by the ABAQUS solver once per each integration point during each time increment. During each call of the subroutine, the rate of deformation, the current mass density, the stress state and the values of the material state variables at the end of the previous time increment are passed to the subroutine, which is tasked with updating the stress state and the state variables, at the end of the current time increment.

Application and validation of the newly developed and implemented polyurea material model is presented in the next section in which an analysis is carried out of a prototypical blast-impact problem.

3. Polyurea blast-impact analysis

3.1 Problem formulation

In this section, the newly developed polyurea material model is used in the computational investigation of blast-impact onto (and the generation and propagation of shock waves within) a polyurea structure. The objective of the analysis was to establish the extent of dissipation of the internal and kinetic energy as a function of polyurea molecular-level and domain-level microstructure.

3.2 Computational model and analysis

Geometrical model. Since in most applications polyurea is used as a ca. 10 mm thick external coating or internal lining, all the calculations carried out in the present work involved 10 mm thick rectangular parallelepiped-shaped polyurea structures.

In the analysis, blast-loading is applied to one of the parallelepiped faces normal to the through-the-thickness direction. Due to the impulsive nature of loading, the resulting shock wave within polyurea is assumed to be of a pure longitudinal character. In other words, the effect of stress waves generated (as a result of the Poisson's effect) at the lateral faces of the polyurea structure is ignored. This assumption is generally valid in the central region of large surface area polyurea coatings. In the computational analysis used, this condition is achieved by applying zero-strain boundary conditions along the directions orthogonal to the shock wave propagation direction. It should be noted that the use of these boundary conditions prevents the development of shear strains, and, hence, the resulting stress state is of a purely normal character. It should be also noted that due to the use of this type of boundary conditions, the dimensions of the computational domain in the lateral directions are immaterial.

Meshed model. The geometrical model is meshed in the through-the-thickness direction using 100 first-order reduced-integration continuum hexahedron elements of equal (0.1 mm) thickness. A schematic of the meshed model used is shown in Figure 9(a). In Figure 9(b), a zoomed-out view of the same computational model is shown along with a square symbol denoting the location of the blast-producing detonation charge.

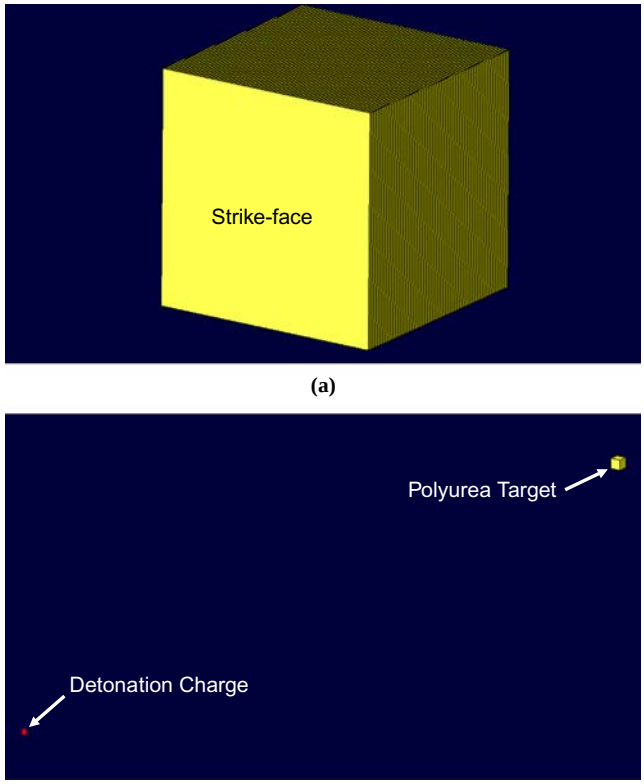

Figure 9.
(a) A schematic of the polyurea structure meshed model used in the present work and (b) zoomed-out view of the same computational model with a square symbol denoting the location of the blast-producing detonation charge

Material model. To describe the thermo-mechanical response of polyurea under blast-loading conditions, the material model newly developed, parameterized and implemented in the user-material subroutine is used.

Initial conditions. The computational domain is assumed to be initially stress-free and quiescent (zero velocity).

Boundary conditions. Until recently, most computational and experimental investigations dealing with the problem of mild Traumatic Brain Injury (m-TBI, of interest in the present work) included blast-wave incident peak overpressures in a 5-20 atm range (Nyein *et al.*, 2010; Amini *et al.*, 2010). It is currently believed that these pressure levels are responsible for more severe TBI cases and that peak overpressures around 1 atm should be investigated in the case of m-TBIs. Consequently, all the calculations carried out in the present work involved an incident peak overpressure of 1 atm. It should be noted, however, that in our ongoing work, the same calculations are extended to higher pressures, of up to several tens of atms. Such pressure levels are of interest in the situations in which polyurea is used to protect structures such as buildings, bridges and/or vehicles from the blasts of higher intensities than the one analyzed in the present work.

Blast-loading is applied using the CONWEP blast-loading algorithm available within ABAQUS/Explicit and originally developed by the US Army Corps of Engineers (Hyde, 1988). Within CONWEP, all the incident and reflected blast-loading parameters are assumed to be functions of a scaled distance (defined as a ratio of (i) the distance between the loaded surface and the explosive charge centroid, and (ii) a cube root of the TNT equivalent explosive charge mass). In the present analysis (1 atm peak overpressure) CONWEP loading is applied to one external face (normal to the through-the-thickness direction) of the computational domain and the evolution of the resulting shock wave monitored in small time increments. It should be noted that the same peak overpressure can be obtained through a different combination of the explosive-charge mass and the standoff distance. While each of these charge-mass/standoff-distance combinations yields the same value of the peak overpressure, temporal evolution of the pressure is different in each case. Consequently, to completely define CONWEP-type loading, it is not sufficient to only define the peak overpressure but also the combination of the charge-mass/standoff-distance which was used to get this overpressure. In the present work, a standoff distance of 1 mm was used and the explosive-charge mass adjusted to obtain the peak overpressure of 1 atm at the target surface.

The remaining boundary conditions, as mentioned above, involve the application of zero-velocity constraints to the lateral faces of the computational domain.

Computational procedure. Explicit, transient, non-linear-dynamics finite element analysis is employed while ensuring that the stability criterion is met through the proper and adaptive selection of the time increment. As mentioned earlier, all the calculations carried out in the present work were performed using ABAQUS/Explicit (Dassault Systems, 2010).

3.3 Results and discussion

In this section, typical results obtained in the aforementioned blast-impact computational investigation using the newly developed polyurea material model are presented and analyzed. The main objective of the analysis is to establish performance criteria and metrics that can be used to assess the shock-mitigation capabilities of polyurea as a function of its soft segment molecular weight and curing temperature.

The findings obtained are used to carry out a preliminary material-selection procedure in order to identify the rendition of polyurea which possesses the highest capacity for mitigation of the blast-impact-induced shock waves.

Typical results. As mentioned earlier, blast impact onto the polyurea strike-face creates a longitudinal shock wave within the polyurea computational domain. The presence of such a shock wave is seen in Figure 10(a)-(c), which show variation of the axial stress through-the-thickness of the polyurea computational domain at post blast-impact times of 1.5, 3.0 and 4.5 μs, respectively. Examination of these figures reveals that the shock wave advances to the right and nearly reaches the free end of the polyurea computational domain at a post-impact time of 4.5 μs. Also, a fairly constant axial stress level is found in the as-shocked (behind the wave-front) portion of the polyurea structure. The finding related to the constant level of stress in the as-shocked portion of polyurea is entirely consistent with the "fully-supported" character of blast loading at very short post-detonation times. It should be noted that the results shown in Figure 10 are obtained using the original polyurea material model, as reported by Amirkhizi *et al.* (2006). Qualitatively similar results are obtained using the newly developed polyurea material model. On the other hand, the subsequent results presented in this manuscript are all generated using the newly developed polyurea material model. It should be recalled that the newly developed polyurea material model allows the inclusion of the effects of polyurea chemistry (e.g. soft-segment molecular weight) and the synthesis route (i.e. curing temperature) on the dynamic mechanical response of this material. These effects are not accounted for in the original polyurea material model, as reported by Amirkhizi *et al.* (2006). The as-shocked axial-stress level is seen to be $\sim$0.28 MPa, which indicates an amplification factor of approximately 2.8 for the employed 1 atm (= 0.1013 MPa) incident blast wave. This finding is consistent with the anticipated value (near 2.0) of the amplification factor in the weak-shock regime (Davison, 2008).

The average shock speed is determined by dividing the distance advanced by the shock-front by the elapsed time. The value obtained is in the 1900-2000 m/s range,

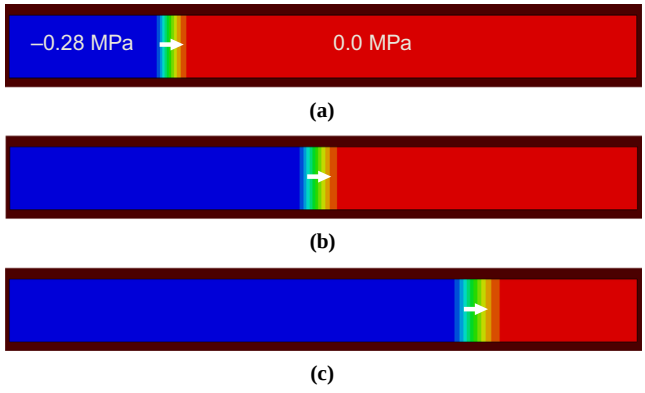

Note: The results are obtained using the original polyurea material model

Source: Amirkhizi *et al.* (2006)

Figure 10.
Variation of the axial stress through-the-thickness of the polyurea computational domain at post blast-impact times of (a) 1.5, (b) 3.0 and (c) 4.5 μs

which is fully consistent with the experimental values in the weak-shock regime as reported by Mock *et al.* (2009). The foregoing findings suggest that the original polyurea material model, as reported by Amirkhizi *et al.* (2006) (and the newly developed material model) can account reasonably well for the expected and observed behavior of the blast-impact-induced shock waves.

Performance metrics identification. Examination of the results shown in Figure 10 shows that the shock-front is not of a discontinuous character, but rather of a finite width and continuous. It should be noted that a numerical bulk viscosity algorithm was not used to increase robustness in the computational procedure. Hence, shock-wave front spreading has to be attributed fully to the operation of viscoelastic and volumetric plastic energy-dissipative processes. When polyurea is used as a protective coating, the width of the shock wave controls the rate of loading experienced by the protected structure. Bearing this in mind, the first metric used to quantify the shock mitigation capacity of polyurea is the width of the shock-wave front. For practical purposes this width is defined as the axial distance between the points on the shock front associated with 1 and 99 percent of the as-shocked axial stress level.

Generation and propagation of the blast-impact-induced shock wave produces internal strain energy and the kinetic energy in the portion of the polyurea swept by the shock. As a result of the operation of energy-dissipative and energy-storing processes, a portion of the internal energy and kinetic energy is extracted from the shock and either converted into heat or into the material defects (including the formation of a new phase(s)). Taking this observation into account, the second (and the last) metric used to quantify the shock-mitigation capacity of polyurea is the fraction of the sum of the internal-strain and kinetic energies which is dissipated/absorbed by polyurea.

Material-selection procedure. Now that two metrics for shock-mitigation capacity of polyurea are defined, one can begin to identify the optimal combination of the polyurea soft-segment molecular weight and the curing temperature which renders a maximum shock-mitigation capacity to polyurea. The results of this procedure are shown in Figure 11(a) and (b) in which the combined effects of the soft-segment molecular weight and curing temperature on the shock width and on the fraction of energy dissipated/stored are shown, respectively. Examination of the results displayed in these figures reveals that polyureas based on the largest soft segment molecular weight and cured at the highest temperatures are characterized by the largest shock-mitigation capacity. These results are reasonable considering the fact that the largest contribution to the shock-mitigation capacity of polyurea is credited to the constrained SS (the α_2 relaxation process) and the volume fraction of these segments increases with an increase in the degree of nano-phase segregation (as pointed out earlier, both an increase in the soft segment molecular weight and in the curing temperature give rise to an increase in the degree of nano-phase segregation). It should be noted, in passing, that in the ongoing computational investigation (the results will be reported in a separate communication), polyureas with intermediate values of the soft segment molecular weight and the curing temperature are found to give rise to a maximum ballistic-protection performance. This finding suggests that different polyurea formulations should be used in blast- and ballistic-protection applications.

It should be recalled that, since in most applications polyurea is used as an external coating or internal lining, all the calculations involved 10 mm thick polyurea

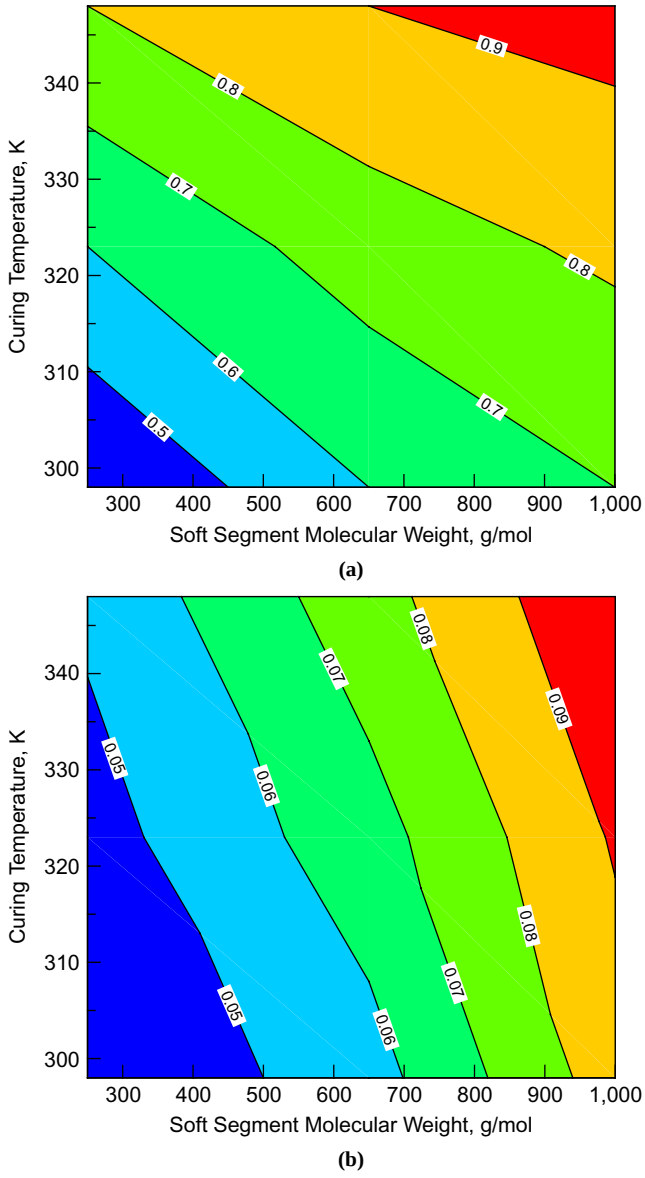

Figure 11.
The effect of the polyurea soft segment molecular weight and curing temperature on (a) the shock width (mm) and (b) the fraction of energy dissipated/stored (no units)

structures (i.e. structures with a thickness comparable to a prototypical helmet external coating/internal lining). A few calculations were also carried out involving thicker polyurea structures, and it is found that the shock-attenuation/dispersion capability of polyurea increases with the thickness of the test structure.

Examination of the results shown in Figure 11(a) and (b) shows that relatively modest shock-attenuation/dispersion benefits are offered by polyurea. This is not

surprising, considering the fact that, at the peak-overpressure levels of 1 atm, the stress wave behaves more as an elastic sound wave rather than as a dissipative shock wave. In our ongoing work, which involves higher peak overpressures, it is being observed that in the presence of true shock waves, polyurea acts as a more potent shock-attenuation/dispersion medium. Under such conditions, it is found that polyurea outperforms its elastomeric competitors such as polyurethane.

Materials-by-design. In the present work, transient non-linear dynamics computational analyses of a blast-loaded polyurea rectangular parallelepiped structure are carried out in order to identify the combination of polyurea chemistry and synthesis route (both affect molecular-level and domain-level microstructure) which imparts the maximum shock-mitigation capacity to this material. This is an example of the so-called "materials-by-design" approach within which component-level performance results are used to guide the identification, design and development of the materials with superior performance needed in the specific application (blast-impact protection of the target structures, in the present case). It should be observed that under the blast-loading conditions of interest to the TBI problem, the results obtained in the present work reveal relatively unimpressive shock-mitigation/dispersion capacity of polyurea. Consequently, one must raise the question if the use of polyurea-based helmet coatings and linings is the best route for prevention of the blast-induced TBI. The results obtained in our ongoing work involving higher peak overpressures, as mentioned above, show that polyurea is very effective in mitigating and attenuating medium to strong shock waves.

4. Summary and conclusions

Based on the results obtained in the present work, the following main summary remarks and conclusions can be drawn:

(1) A new physically-based, microstructure- and synthesis-route-dependent material model for nano-segregated polyurea is developed.

(2) Two aspects of polyurea microstructure are included in the present model:
   - molecular-weight-controlled soft-segment chain-length; and
   - the extent and morphology of hard-domain nano-segregates (hard domains).

   These aspects of polyurea microstructure are, in turn, related to the material chemistry and synthesis route.

(3) Available experimental and theoretical data are used to parameterize various aspects of the newly developed material model. The model is next validated by comparing its predictions for some material-microstructure-dependent properties (e.g. shock speed) against their experimental counterparts.

(4) Transient non-linear dynamics computational analyses of the blast impact onto a polyurea structure are next used to define two metrics quantifying polyurea's shock-mitigation capability.

(5) Lastly, a material-selection procedure is used in order to identify optimum formulation of polyurea with respect to its blast-mitigation performance. The results obtained are used to demonstrate the so-called "materials-by-design" approach within which the component/system-level performance is used to guide the design and development of the optimum constituent material(s).

References

Amini, M.R., Simon, J. and Nemat-Nasser, S. (2010), "Numerical modeling of effect of polyurea on response of steel plates to impulsive loads in direct pressure pulse experiments", *Mechanics of Materials*, Vol. 42, pp. 615-627.

Amirkhizi, A.V., Isaacs, J., McGee, J. and Nemat-Nasser, S. (2006), "An experimentally-based viscoelastic constitutive model for polyurea, including pressure and temperature effects", *Philosophical Magazine*, Vol. 86, pp. 5847-5866.

Arruda, E.M. and Boyce, M.C. (1993), "A three-dimensional constitutive model for the large stretch behavior of elastomers", *Journal of Mechanics and Physics of Solids*, Vol. 41, pp. 389-412.

Bogoslovov, R.B., Roland, C.M. and Gamache, R.M. (2007), "Impact-induced glass-transition in elastomer coatings", *Applied Physics Letters*, Vol. 90, pp. 221910-221913.

Bonart, R. and Müller, E.H. (1974), "Phase separation in urethane elastomers as judged by low-angle X-ray scattering. I. Fundamentals", *Journal of Macromolecular Science, Part B: Physics*, Vol. 10, pp. 177-189.

Castagna, A.M., Pangon, A., Choi, T., Dillon, G.P. and Runt, J. (2012), "The role of soft segment molecular weight on microphase separation and dynamics of bulk polymerized polyureas", *Macromolecules*, October.

Choi, T., Fragiadakis, D., Roland, C.M. and Runt, J. (2012), "Microstructure and segmental dynamics of polyurea under uniaxial deformation", *Macromolecules*, Vol. 45, pp. 3581-3589.

Choi, T., Weksler, J., Padsalgikar, A. and Runt, J. (2009), "Influence of soft segment composition on phase-separated microstructure of polydimethylsiloxane-based segmented polyurethane copolymers", *Polymer*, Vol. 50, pp. 2320-2327.

Das, S., Yilgor, I., Yilgor, E. and Wilkes, G.L. (2008), "Probing the urea hard domain connectivity in segmented, non-chain extended polyureas using hydrogen-bond screening agents", *Polymer*, Vol. 49, pp. 174-179.

Das, S., Cox, D., Wilkes, G., Klinedinst, D., Yilgor, I. and Yilgor, E. (2007a), "Effect of symmetry and H-bond strength of hard segments on the structure-property relationships of segmented, nonchain extended polyurethanes and polyureas", *Journal of Macromolecular Science, Part B: Physics*, Vol. 46, pp. 853-875.

Das, S., Yilgor, I., Yilgor, E., Inci, B., Tezgel, O., Beyer, F.L. and Wilkes, G.L. (2007b), "Structure – property relationships and melt rheology of segmented, non-chain extended polyureas: effect of soft segment molecular weight", *Polymer*, Vol. 48, pp. 290-301.

Dassault Systems (2010), *ABAQUS Version 6.10 EF1, User Documentation*, Dassault Systems, Providence, RI.

Davison, L. (2008), *Fundamentals of Shock-Wave Propagation in Solids*, Springer, Berlin.

El-Sayed, T.M. (2008), "Constitutive models for polymers and soft biological tissues", unpublished doctoral dissertation, California Institute of Technology, Pasadena, CA.

Garrett, J.T., Lin, J.S. and Runt, J. (2002), "Influence of preparation conditions on microdomain formation in poly(urethane urea) block copolymers", *Macromolecules*, Vol. 35, pp. 161-168.

Garrett, J.T., Runt, J. and Lin, J.S. (2000), "Microphase separation of segmented poly(urethane urea) block copolymers", *Macromolecules*, Vol. 33, pp. 6353-6359.

Garrett, J.T., Siedlecki, C.A. and Runt, J. (2001), "Microdomain morphology of poly(urethane urea) multiblock copolymers", *Macromolecules*, Vol. 34, pp. 7066-7070.

Garrett, J.T., Xu, R., Cho, J. and Runt, J. (2003), "Phase separation of diamine chain-extended poly(urethane) copolymers: FTIR spectroscopy and phase transitions", *Polymer*, Vol. 44, pp. 2711-2719.

Grujicic, M. and Pandurangan, B. (2012), "Meso-scale analysis of segmental dynamics in micro-phase segregated polyurea", *Journal of Materials Science*, Vol. 47, pp. 3876-3889.

Grujicic, M., He, T. and Pandurangan, B. (2011a), "Development and parameterization of an equilibrium material model for segmented polyurea", *Multidiscipline Modeling in Materials and Structures*, Vol. 7, pp. 96-114.

Grujicic, M., He, T. and Pandurangan, B. (2011b), "Development and parameterization of a time-invariant (equilibrium) material model for segmented elastomeric polyureas", *Journal of Materials: Design and Applications*, Vol. 225, pp. 182-194.

Grujicic, M., Bell, W.C., Pandurangan, B. and Glomski, P.S. (2011c), "Fluid/structure interaction computational investigation of the blast-wave mitigation efficacy of the advanced combat helmet", *Journal of Materials Engineering and Performance*, Vol. 20, pp. 877-893.

Grujicic, M., Bell, W.C., Pandurangan, B. and He, T. (2010a), "Blast-wave impact-mitigation capability of polyurea when used as helmet suspension pad material", *Materials and Design*, Vol. 31, pp. 4050-4065.

Grujicic, M., Pandurangan, B., Koudela, K.L. and Cheeseman, B.A. (2006), "A computational analysis of the ballistic performance of light-weight hybrid-composite armors", *Applied Surface Science*, Vol. 253, pp. 730-745.

Grujicic, M., Arakere, A., Pandurangan, B., Grujicic, A., Littlestone, A.A. and Barsoum, R.S. (2012a), "Computational investigation of shock-mitigation efficacy of polyurea when used in a combat helmet: a core sample analysis", *Multidiscipline Modeling in Materials and Structures*, Vol. 8, pp. 297-331.

Grujicic, M., d'Entremont, B.P., Pandurangan, B., Runt, J., Tarter, J. and Dillon, G. (2011d), "Concept-level analysis and design of polyurea for enhanced blast-mitigation performance", *Journal of Materials Engineering and Performance*, Vol. 21, pp. 2024-2037.

Grujicic, M., He, T., Pandurangan, B., Svingala, F.R., Settles, G.S. and Hargather, M.J. (2011e), "Experimental characterization and material-model development for microphase-segregated polyurea: an overview", *Journal of Materials Engineering and Performance*, Vol. 21, pp. 2-16.

Grujicic, M., Pandurangan, B., Arakere, G., Bell, W.C., He, T. and Xie, X. (2010b), "Material-modeling and structural-mechanics aspects of the traumatic brain injury problem", *Multidiscipline Modeling in Materials and Structures*, Vol. 6, pp. 335-363.

Grujicic, M., Pandurangan, B., Bell, W.C., Cheeseman, B.A., Yen, C.-F. and Randow, C.L. (2011f), "Molecular-level simulations of shock generation and propagation in polyurea", *Materials Science and Engineering A*, Vol. 528, pp. 3799-3808.

Grujicic, M., Pandurangan, B., He, T., Cheeseman, B.A., Yen, C.-F. and Randow, C.L. (2010c), "Computational investigation of impact energy absorption capability of polyurea coatings via deformation-induced glass transition", *Materials Science and Engineering A*, Vol. 527, pp. 7741-7751.

Grujicic, M., Pandurangan, B., King, A.E., Runt, J., Tarter, J. and Dillon, G. (2011g), "Multi-length scale modeling and analysis of microstructure evolution and mechanical properties in polyurea", *Journal of Materials Science*, Vol. 46, pp. 1767-1779.

Grujicic, A., LaBerge, M., Grujicic, M., Pandurangan, B., Runt, J., Tarter, J. and Dillon, G. (2012b), "Potential improvements in shock-mitigation efficacy of a polyurea-augmented advanced combat helmet: a computational investigation", *Journal of Materials Engineering and Performance*, Vol. 21, pp. 1562-1579.

Grujicic, M., Yavari, R., Snipes, J.S., Ramaswami, S., Runt, J., Tarter, J. and Dillon, G. (2012c), "Molecular-level computational investigation of shock-wave mitigation capability of polyurea", *Journal of Materials Science*, Vol. 47, pp. 8197-8215.

Grujicic, M., d'Entremont, B.P., Pandurangan, B., Grujicic, A., LaBerge, M., Runt, J., Tarter, J. and Dillon, G. (2012d), "A study of the blast-induced brain white-matter damage and the associated diffuse axonal injury", *Multidiscipline Modeling in Materials and Structures*, Vol. 8, pp. 213-245.

Hernandez, R., Weksler, J., Padsalgikar, A. and Runt, J. (2007), "Microstructural organization of three-phase polydimethylsiloxane-based segmented polyurethanes", *Macromolecules*, Vol. 40, pp. 5441-5449.

Hernandez, R., Weksler, J., Padsalgikar, A., Choi, T., Angelo, E., Lin, J.S., Xu, L.C., Siedlecki, C.A. and Runt, J. (2008), "A comparison of phase organization of model segmented polyurethanes with different intersegment compatibilities", *Macromolecules*, Vol. 41, pp. 9767-9776.

Hyde, D. (1988), *User's Guide for Microcomputer Programs, CONWEP and FUNPRO – Applications of TM 5-855-1*, US Army Engineer Waterways Experimental Station, Vicksburg, MS.

Jiao, T., Clifton, R.J. and Grunschel, S.E. (2009), "Pressure-sensitivity and constitutive modeling of an elastomer at high strain rates", *Shock Compression of Condensed Matter 2009: Proceedings of the American Physical Society Topical Group on Shock Compression of Condensed Matter*, American Institute of Physics, Melville, NY, pp. 1229-1232.

Leung, L.M. and Koberstein, J.T. (1985), "Small-angle scattering analysis of hard-microdomain structure and microphase mixing in polyurethane elastomers", *Journal of Polymer Science: Polymer Physics Edition*, Vol. 23, pp. 1883-1913.

Li, C. and Lua, J. (2009), "A hyper-viscoelastic constitutive model for polyurea", *Materials Letters*, Vol. 63, pp. 877-880.

Matthews, W. (2004), "Polymer protection", *Defense News*, April, pp. 32-35.

Mock, W., Bartyczak, S., Lee, G., Fredderly, J. and Jordan, K. (2009), "Dynamic properties of polyurea-1000", *Shock Compression of Condensed Matter 2009: Proceedings of the American Physical Society Topical Group on Shock Compression of Condensed Matter*, American Institute of Physics, Melville, NY, pp. 1241-1244.

Nyein, M.K., Jason, A.M., Yu, L., Pita, C.M., Joannopoulos, J.D., Moore, D.F. and Radovitzky, R.A. (2010), "In silico investigation of intracranial blast mitigation with relevance to military traumatic brain injury", *Proceedings of the National Academy of Sciences, USA*, Vol. 48, pp. 20703-20708.

Ogden, R.W. (1972), "Large deformation isotropic elasticity – on the correlation of theory and experiment for incompressible rubberlike solids", *Proceedings of the Royal Society of London A*, Vol. 326, pp. 565-584.

Ortiz, M. and Molinari, A. (1992), "Effect of strain-hardening and rate sensitivity on the dynamic growth of a void in a plastic material", *Journal of Applied Mechanics – Transactions of the ASME*, Vol. 59, pp. 48-53.

Pipkin, A.C. (1972), *Lectures on Viscoelasticity Theory*, Springer, New York, NY.

Porter, J.R., Dinan, R.J., Hammons, M.I. and Knox, K.J. (2002), "Polymer coatings increase blast resistance of existing and temporary structures", *AMPTIAC Quarterly*, Vol. 6 No. 4, pp. 47-52.

Qi, H.J. and Boyce, M.C. (2005), "Stress-strain behavior of thermoplastic polyurethanes", *Mechanics of Materials*, Vol. 37, pp. 817-839.

Ryan, A.J. (1989), "Spinodal decomposition during bulk copolymerization: reaction injection molding", *Polymer*, Vol. 31, pp. 707-712.

Sheth, J.P., Aneja, A., Wilkes, G.L., Yilgor, E., Atilla, G.E., Yilgor, I. and Beyer, L. (2004), "Influence of system variables on the morphology and dynamic mechanical behavior of polydimethylsiloxanebased segmented polyureathane and polyurea copolymers: a comparative perspective", *Polymer*, Vol. 45, pp. 6919-6932.

Weinberg, K., Mota, A. and Ortiz, M. (2006), "A variational constitutive model for porous metal plasticity", *Computational Mechanics*, Vol. 37, pp. 142-152.

Williams, M.L., Landel, R.F. and Ferry, J.D. (1955), "The temperature dependence of relaxation mechanisms in amorphous polymers and other glass-forming liquids", *Journal of American Chemical Society*, Vol. 77, pp. 3701-3707.

About the authors

Mica Grujicic is a Professor, Mechanical Engineering, Clemson University. Mica Grujicic's research interests include computational engineering. Mica Grujicic is the corresponding author and can be contacted at: gmica@clemson.edu

Jennifer Snipes is a post-doctoral Fellow, Mechanical Engineering, Clemson University. Jennifer Snipes' research interests include computational material modeling.

Subrahmanian Ramaswami is a post-doctoral Fellow, Mechanical Engineering, Clemson University. Subrahmanian Ramaswami's research interests include computational material modeling.

Rohan Galgalikar is a doctoral student, Mechanical Engineering, Clemson University. Rohan Galgalikar's research interests include shock propagation.

James Runt is a Professor of polymer science, the Department of Material Science and Engineering, Pennsylvania State University. James Runt's research interests include synthesis and characterization of advanced polymeric materials.

James Tarter is Head of the Advanced Computational Analysis and Design Department in the Composite Materials Division, Applied Research Laboratories, Pennsylvania State University. James Tarter's research interests include advanced computational analysis of materials response under extreme loading conditions.